

Electronic structure and vacancy formation of Li₃N

Shunian Wu,^{1,2} Zhili Dong,² Freddy Boey,² and Ping Wu^{1,2,a)}

¹Institute of High Performance Computing, 1 Fusionopolis Way, No. 16-16 Connexis, Singapore 138632, Singapore

²School of Materials Science and Engineering, Nanyang Technological University, Nanyang Avenue, Singapore 639798, Singapore

(Received 24 January 2009; accepted 7 April 2009; published online 29 April 2009)

The electronic structure and vacancy formation of Li₃N were studied using first principles methods. We found Li₃N exhibits strong ionic character with slight covalent bonding between N and Li. The Li vacancy formation energy decreases with an increase in nitrogen partial pressure, while the N vacancy formation energy increases with increasing nitrogen partial pressure. The Li(2) site vacancy is found to have the lowest formation energy under nitrogen-rich conditions. Formation of $V_{\text{Li}(2)}^-$ brings about delocalization of valence electrons, and reduces the band gap by 0.2 eV. These results suggest potential ways to enhance vacancy concentration in Li₃N for higher ionic conductivity.
© 2009 American Institute of Physics. [DOI: 10.1063/1.3126449]

Li₃N has an exceptionally large Li ionic conductivity due to intrinsic defects and the resulting hopping of Li ions from occupied Li sites into unoccupied ones.¹ The nature of the defect plays a critical role in the understanding and application of the material for hydrogen storage and lithium batteries. Li₃N can be described as a sequence of Li(1) and Li(2)₂N layers perpendicular to *c* in space group *P6/mmm* (Fig. 1). Earlier x-ray diffraction and powder neutron diffraction studies reported 1~2% vacancies in Li(2) position at room temperature.^{1,2} The vacancy concentration can go up to 4% at high temperature. Conversely, recent powder neutron diffraction analysis found no Li vacancies in the temperature range of 20–673 K.³ This contradiction is attributed to different crystal growing procedures. Clearly, a fundamental understanding of the nature of the vacancy and the impact of Li₃N growth environment is necessary to optimize crystal growth conditions for high concentration of vacancy in Li₃N.

Although the electronic properties of Li₃N have been studied extensively,^{4–7} research on its defect properties is limited. A lattice energy program simulation showed that an interstitial defect cannot form in the structure.⁸ The energetically favorable vacancy comes from Li(2) removal. Sarnthein *et al.*⁹ asserted that Li(2) vacancy must be formed in a charged state based on the band structure. An uncharged Li(2) vacancy would bring about a hole in the valence band and result in an energetically very unfavorable N²⁻ ion. There is, to date, a paucity of data for quantitative comparison of the formation energy of various vacancies. In addition, the effect and role of the crystal growth environment are not established. Therefore, we investigate the formation energies of all major intrinsic vacancies in Li₃N under different atmospheric conditions using first-principles calculations. We also attempt to establish the relationship between the fabrication conditions and vacancy formation mechanism.

First-principles calculations were performed using density functional theory and the projector augmented wave method as implemented in VASP.^{10–12} For the exchange correlation, we employed the generalized-gradient approxima-

tion (GGA) parameterized by Perdew *et al.*^{13,14} In our pseudopotential, 2*s* and 2*p* for Li and 2*s* and 2*p* for N were treated as valence. All atoms in the supercells were free to move in the geometry optimization. The electronic structure of the perfect Li₃N crystal was investigated with primitive cell and 11×11×11 *k*-point mesh according to the Monkhorst–Pack scheme.¹⁵ The optimized lattice constants *a*=3.65 Å and *c*=3.88 Å are consistent with the experimental values, 3.64 and 3.87 Å.^{2,3} Li₃N supercells of 108 atoms were constructed for vacancy calculations by 3×3×3 expansion of the unit cell. 4×4×4 *k*-points (the Monkhorst–Pack method) were selected in supercell calculations. Convergence with respect to *k*-points and energy cutoff was checked during all calculations.

The formation energy of a charged vacancy $E_F(V^q)$ is defined as

$$E_F(V^q) = E_T(V^q) - E_T(\text{bulk}) + \mu_i + q(\text{VBM} + \Delta V + \varepsilon_F), \quad (1)$$

where $E_T(\text{bulk})$ and $E_T(V^q)$ are the total energy of the defect-free supercell and the supercell with vacancy at charge state *q*, respectively; μ_i is the chemical potential of the atom removed from the supercell to form the vacancy; ε_F is the Fermi energy measured with reference to the valence band maximum (VBM). The correction term ΔV aligns the refer-

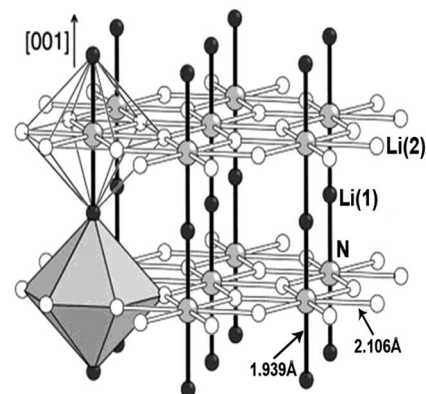


FIG. 1. Crystal structure of Li₃N.

^{a)}Author to whom correspondence should be addressed. Electronic mail: wuping@ihpc.a-star.edu.sg. FAX: 65-64632536.

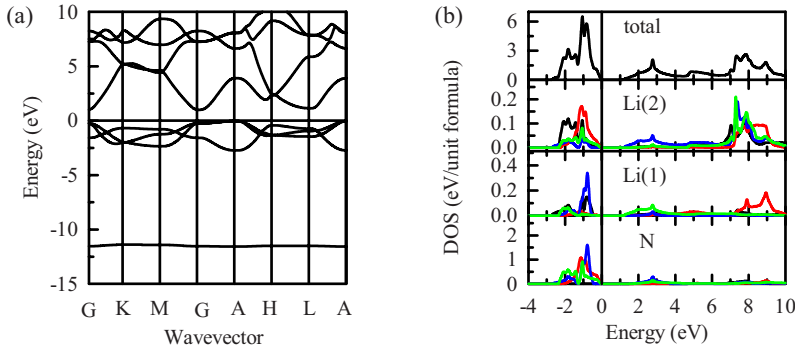


FIG. 2. (Color online) Calculated electronic band structure (a) and DOS for defect-free Li_3N (b). The local partial DOS components in (b) are: s black, p_x red, p_y blue, and p_z green. The Fermi level is set to zero energy.

ence potential in the defect supercell with that in the defect-free supercell.^{16,17}

The chemical potential μ_i depends on crystal growth conditions such as the nitrogen partial pressure. The valid range of N_2 partial pressure P_{N_2} is determined by Li_3N formation enthalpy $\Delta H_f^{\text{Li}_3\text{N}}$

$$\frac{\Delta H_f^{\text{Li}_3\text{N}}}{kT} \leq \ln P_{\text{N}_2} \leq 0 \quad \text{with} \quad \Delta H_f^{\text{Li}_3\text{N}} = 3(\mu_{\text{Li}} - \mu_{\text{Li}}^o) + (\mu_{\text{N}} - \mu_{\text{N}}^o), \quad (2)$$

where μ_{Li} and μ_{N} are the chemical potential of Li and N in Li_3N , respectively; μ_{Li}^o and μ_{N}^o are the energy of metallic Li and gaseous N_2 (per nitrogen atom) in the standard state; k is the Boltzmann constant; and T is the temperature. The Li_3N formation enthalpy is calculated to be -1.59 eV per Li_3N , which is within the typical GGA errors from experimental value of -1.73 eV per Li_3N .¹⁸

The calculated electronic band structure and density of states (DOS) of the defect-free Li_3N are shown in Fig. 2. The VBM and conduction band minimum (CBM) are located at A and Γ , separately, giving an indirect gap consistent with previous experimental and theoretical reports.^{4,6,9} The calculated band gap is 1.1 eV, which is underestimate by 1.1 eV as compared with the measured value.¹⁹ The band around -11.5 eV is dominated by N $2s$ state with a Li $2s$ and $2p$ admixture. The conduction bands are mainly composed of Li $2s$ and $2p$ states and the occupied valence bands originate from N $2s$ and $2p$ states. The partial overlapping of Li $2s$ state with N $2p$ state in the valence band region suggests possible Li(1)–N and Li(2)–N s - p covalent bonds. The different characteristics of p_x , p_y , and p_z states of N atom indicate the anisotropy of the structure. Employing Bader’s “atoms in molecules” scheme,²⁰ we obtained nominal valences of $\text{N}^{-2.44}$, $\text{Li}(1)^{+0.82}$, and $\text{Li}(2)^{+0.81}$. This further suggests covalent bonding between Li and N. This is consistent with the real-space full-multiple-scattering (RSFMS) calculations by Fister *et al.*⁷

The formation energies of all major intrinsic vacancies in Li(1), Li(2), and N sites calculated with Eq. (1) as a function of Fermi level at N-rich condition (i.e., $\mu_{\text{N}} = \mu_{\text{N}}^o$). The Li(2) site vacancies are located in N-containing layers, while the Li(1) site vacancies lie in the layers between these N-containing layers (Fig. 1). Li(2) site vacancy shows the lowest formation energy, which is consistent with experimental observations.^{2,3} The negative $V_{\text{Li}(2)}^-$ vacancy is the most abundant vacancy with the formation energy as low as -1.5 eV, indicating that thermal generation of vacancies is important even at low temperature in agree-

ment with experimental report.¹ The high concentration of Li(2) site vacancy is believed to contribute significantly to the unusually large ionic conductivity of Li_3N since it provides pathways for Li ion hopping. An increase in Li vacancy concentration corresponds to high Li ion mobility and thus high ionic conductivity.²¹ The vacancy formation energy in the Li(1) site is about 1.7 eV higher than that in the Li(2) site. Therefore, removal of the lithium between the Li_2N layers is a very energetically unfavorable process since the two nearly triply negative nitrogen ions would now be repelled by their own ionic charges and by the effective negative charge of $V_{\text{Li}(1)}^-$ vacancy. The formation energy of neutral nitrogen vacancies is the highest. Even the most stable V_{N}^{3+} vacancy among possible N vacancies has a formation energy that is about 1.0 eV higher than that of $V_{\text{Li}(2)}$. This indicates that the nitrogen vacancies rarely exist under N-rich conditions.

The vacancy formation energy as a function of nitrogen partial pressure is shown in Fig. 4 for two characteristic Fermi levels, VBM and CBM. Atmospheric nitrogen conditions determine the type and concentration of vacancies in Li_3N . When the Fermi energy is set at the VBM, V_{N}^{3+} and $V_{\text{Li}(2)}$ may form. The difference in formation energy of V_{N}^{3+} and V_{N}^{2+} is only 0.01 eV, and consequently they have similar concentrations. The formation energy of N vacancies increases with an increase in nitrogen partial pressure, while the formation energy of Li vacancies decreases with an in-

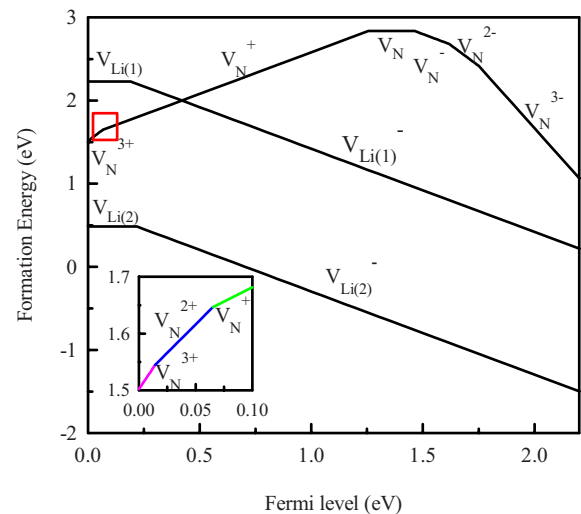


FIG. 3. (Color online) Vacancy formation energies as a function of the Fermi level ϵ_F at nitrogen-rich condition. The inset is a zoomed view of the highlighted rectangle area. The zero energy of ϵ_F corresponds to the valence-band maximum.

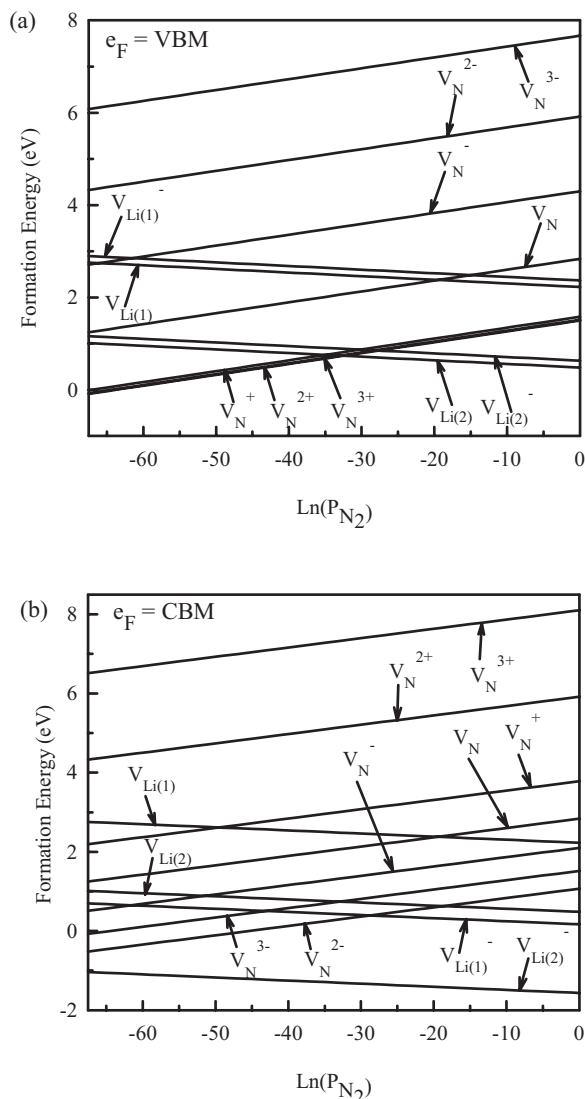


FIG. 4. Vacancy formation energies as a function of nitrogen partial pressure at two typical Fermi level VBM (a) and CBM (b).

crease in nitrogen partial pressure. Therefore, V_{N}^{3+} has the lowest formation energy at low nitrogen partial pressure, while $V_{\text{Li}(2)}$ has the lowest formation energy at high nitrogen partial pressure. The turning point for alternation of dominated vacancy from V_{N}^{3+} to $V_{\text{Li}(2)}$ is at the nitrogen partial pressure slightly above 4.66×10^{-15} Pa. Since such low N partial pressure is unattainable in experiments, this in fact excludes the possibility to form dominating V_{N}^{3+} in the synthesized Li_3N . The formation energy of negative $V_{\text{Li}(2)}$ vacancy is 0.22 eV higher than that of the neutral $V_{\text{Li}(2)}$ vacancy. Evidently, the neutral $V_{\text{Li}(2)}$ vacancy is dominant at high nitrogen partial pressure rather than the negative $V_{\text{Li}(2)}$ vacancy. Therefore, the assertion of exclusive $V_{\text{Li}(2)}$ vacancy by Sarnthein *et al.*⁹ is not supported when the Fermi energy is located at VBM.

When the Fermi energy is set at CBM, the negative $V_{\text{Li}(2)}$ vacancy occurs exclusively in the structure, which is consistent with the assertion by Sarnthein *et al.*⁹ The formation energy of $V_{\text{Li}(2)}$ vacancy decreases greatly from -0.95 eV at low nitrogen partial pressure to -1.50 eV at high nitrogen partial pressure. This results in a remarkable increase in $V_{\text{Li}(2)}$ vacancy level and thus conductivity.

Formation of charged vacancies in Li_3N brings about a significant change in band structure. $V_{\text{Li}(2)}$ vacancy splits the peak at about -11 eV into two peaks with separation of 0.3 eV. The accompanying highly splitted p_x , p_y , and p_z states indicate valence electron delocalization, and thus enhance conductivity.²² The vacancy charge is unevenly distributed among all atoms with the neighboring N atoms allocated the largest portion. This brings about a decrease in the gap between VBM and CBM by -0.2 eV. Conversely, the formation of V_{N}^{3+} in the structure expands the gap by 0.2 eV. The p_x state exhibits moderate splitting, indicating valence electron delocalization in Li_2N layers. This increases the anisotropy of conductivity. The alternation of band structure with vacancy implicates additional controlling of Li_3N conductivity via vacancy selection.

In conclusion, first-principles calculations suggest that vacancies in Li(2) sites are responsible for the experimentally observed apparent nonstoichiometry of Li_3N . The vacancy formation energy at Li(2) sites decreases with an increase in nitrogen partial pressure. Since the vacancies in the Li(2) sites are responsible for the conductivity of Li_3N , nitrogen-rich condition is preferred for Li_3N fabrication process to attain high vacancy concentration and thus conductivity. Under extreme conditions, the dominant $V_{\text{Li}(2)}$ vacancy reaches formation energy as low as -1.50 eV. Such low formation energy suggests that thermal generation of vacancies plays an important role in controlling vacancy level and therefore conductive mechanism. Formation of $V_{\text{Li}(2)}$ brings about valence electron delocalization and thus enhances the ionic conductivity. These results enhance our understanding of the physics of intrinsic defects and potential measure to control the vacancy in Li_3N and its derivatives.

The authors thank Michael Sullivan for critical English proof reading of this letter.

¹H. Schulz and K. H. Thiemann, *Acta Crystallogr., Sect. A: Cryst. Phys., Diff., Theor. Gen. Crystallogr.* **35**, 309 (1979).

²D. H. Gregory, P. M. O'Meara, A. G. Gordon, J. P. Hodges, S. Short, and J. D. Jorgensen, *Chem. Mater.* **14**, 2063 (2002).

³A. Huq, J. W. Richardson, E.R. Maxey, D. Chandra, and W.-M. Chien, *J. Alloys Compd.* **436**, 256 (2007).

⁴G. Kerker, *Phys. Rev. B* **23**, 6312 (1981).

⁵R. Dovesi, C. Pisani, F. Ricca, C. Roetti, and V. R. Saunders, *Phys. Rev. B* **30**, 972 (1984).

⁶P. Blaha, K. Schwarz, and P. Herzig, *Phys. Rev. Lett.* **54**, 1192 (1985).

⁷T. T. Fister, G. T. Seidler, E. L. Shirley, F. D. Vila, J. J. Rehr, K. P. Nagle, J. C. Linehan, and J. O. Cross, *J. Chem. Phys.* **129**, 044702 (2008).

⁸J. R. Walker and C. R. A. Catlow, *J. Phys. (Paris), Colloq.* **41**, C6-32 (1980).

⁹J. Sarnthein, K. Schwarz, and P. E. Blöchl, *Phys. Rev. B* **53**, 9084 (1996).

¹⁰P. E. Blöchl, *Phys. Rev. B* **50**, 17953 (1994).

¹¹G. Kresse and J. Hafner, *Phys. Rev. B* **47**, 558 (1993).

¹²G. Kresse and J. Hafner, *Phys. Rev. B* **49**, 14251 (1994).

¹³J. P. Perdew, K. Burke, and M. Ernzerhof, *Phys. Rev. Lett.* **77**, 3865 (1996).

¹⁴J. P. Perdew, K. Burke, and M. Ernzerhof, *Phys. Rev. Lett.* **78**, 1396 (1997).

¹⁵J. H. Monkhorst and D. J. Pack, *Phys. Rev. B* **13**, 5188 (1976).

¹⁶C. G. Van de Walle and J. Neugebauer, *J. Appl. Phys.* **95**, 3851 (2004).

¹⁷S. B. Zhang, *J. Phys.: Condens. Matter* **14**, R881 (2002).

¹⁸J. Sangster and A. D. Pelton, *J. Phase Equilib.* **13**, 291 (1992).

¹⁹H. Brendecke and W. Bludau, *Phys. Rev. B* **21**, 805 (1980).

²⁰R. Bader, *Atoms in Molecules: A Quantum Theory* (Oxford University Press, New York, 1990).

²¹Z. Stoeva, R. Gomez, A. G. Gordon, M. Allan, D. H. Gregory, G. B. Hix, and J. J. Titman, *J. Am. Chem. Soc.* **126**, 4066 (2004).

²²Y. Che, A. Datar, X. Yang, T. Naddo, J. Zhao, and L. Zang, *J. Am. Chem. Soc.* **129**, 6354 (2007).